Desalination and Water Treatment
www.deswater.com
doi: 10.1080/19443994.2013.769918

51 (2013) 6736–6742
October

Taylor & Francis
Taylor & Francis Group

Fabrication of Al_2O_3/PSf nanocomposite membranes: efficiency comparison of coating and blending methods in modification of filtration performance

Yasaman Mohades Mojtahedi, Mohammad Reza Mehrnia*, Maryam Homayoonfal

School of Chemical Engineering, College of Engineering, University of Tehran, Tehran, Iran
Tel. +98 2161112184; Fax: +98 2166954041; email: mmehrnia@ut.ac.ir

Received 28 November 2012; Accepted 18 January 2013

ABSTRACT

Al_2O_3 nanoparticles were added to polysulfone (PSf) ultrafiltration membrane through the two methods of surface deposition and structure entrapment, to study the membrane performance in filtration of dye solutions. Alumina nanoparticles were synthesized through coprecipitation method and were added to casting solution containing PSf as a main polymer (17 wt.%), *N*-methyl-2-pyrrolidone as a solvent (75 wt.%), and polyethylene glycol with molecular weight of 400 as a pore former (8 wt.%). In addition, a deposition of nanoparticles onto the surface of the pre-prepared PSf membrane was formed by using photo-polymerization method. Water flux and rejection of disperse dye solution were studied afterwards. According to the obtained results, the synthesized nanocomposite membranes showed less flux decline but higher dye rejection in comparison with neat polymeric membranes. Results also showed higher dye rejection for membrane modified by entrapment method, while membrane modified by surface deposition method had higher dye flux. Fourier transform infrared spectrum analysis confirmed the presence of alumina nanoparticles in the structure and on the surface of the membrane. According to X-ray diffraction analysis results, the size of synthesized alumina nanoparticles were 16.61 nm and it reached 58.3 nm after being placed in the polymeric structure.

Keywords: Nanocomposite membrane; Alumina nanoparticles; Surface deposition; Structure blending

1. Introduction

Ultrafiltration and nanofiltration membranes attract the attention of many researchers due to their different applications in water/wastewater treatment especially in dye separation [1]. However, the flux decline caused by fouling is the most important problem in the application of membrane in industrial processes [2]. Membrane fouling is caused by deposition of hydrophobic materials on the surface of membrane during the time [3]. Therefore, increasing hydrophilicity of the membrane by using the presence of hydrophilic particles can be assumed a good solution for modification of the membrane resistance against fouling. In the recent decade, the preparation of organic–inorganic composite membranes with controlled characteristics have been of high interest [4–8].

*Corresponding author.

Development in nanotechnology and materials science on the one hand, and the need for specific separations with high efficiency on the other hand has caused the synthesis of nanocomposite membranes. Membrane structures obtained from the presence of nanoparticles in a polymeric structure can be used as multi-purpose tools because they benefit from the both characteristics of nanoparticles and polymeric matrix at the same time. Nanocomposite membranes have modified mechanical and thermal properties and efficiency comparing to non-modified polymeric membranes. These membranes have the flexibility and reactivity of the polymers and simultaneously, they enjoy thermal and mechanical stability of nanoparticles as well [9]. In case, the synthesis conditions are controlled, nanoparticles are able to be used as an additive to modify the membrane, in addition to giving their specific characteristics to the nanocomposite membrane. Nanocomposite membranes have different properties compared with membranes without nanoparticles to the extent that various nanoparticles are used in different researches to create modification on the polymeric membranes [9,10].

According to previous researches, the presence of nanoparticles usually results in an increase in hydrophilicity and decrease in fouling of polymeric membranes in filtration processes. The presence of TiO_2, ZnO, Al_2O_3 [11,12], ZrO_2, SiO_2, Fe_3O_4, silver, and Fe nanoparticles and fullerene [13] increases mechanical and thermal resistance of polymeric membranes [9]. ZnO [14], TiO_2 [15–25], and Silver [26–29] nanoparticles create antibacterial characteristic in polymeric membranes while ZrO_2 [30,31] and Fe [32,33] give catalytic properties. In addition, conductivity characteristic is caused in polymeric membranes by SiO_2 nanoparticle [34–38] and magnetic characteristic is created by Fe_3O_4 nanoparticle in polymeric membranes [39]. Each of above-mentioned nanoparticles can be pre-synthesized or fabricated in situ in polymeric solution. Taurozzi et al. [29] compared anti biofouling efficiency of nanocomposite membranes containing ex situ and in-situ silver nanoparticles. However, silver compounds (both in ionic and in nanoparticle form) have long been known to own antimicrobial activity by releasing silver ions which react with thiol (–SH) groups in microbial cells or by attaching to cellular membrane of microorganism [27,29], their research showed that in situ synthesized silver nanoparticles are more efficient than ex situ ones in biofouling mitigation. Difference in activity between pre-synthesized and in situ synthesized polysulfone (PSf)/Ag nanocomposite membranes could result from a higher number of smaller nanoparticles, higher total surface area of the filler, higher silver attachment to microorganisms and release to filtration medium, and therefore, higher antibiofouling efficiency [29].

Taking into consideration the hydrophobic nature of the membrane main polymer, PSf, and considering the fouling problem some time after the beginning of the filtration, it seems necessary to add nanoparticles with hydrophilic properties to the membrane. According to the literatures, in spite of investigations about the addition of alumina nanoparticles to some polymeric membrane such as PVDF [11] and PES [12], there is no essential study for PSf membrane. Therefore, pre-synthesized alumina nanoparticles were added in this study to the membrane through the two methods of structure entrapment and surface deposition by using photo-polymerization. Then, the structure and filtration performance of the obtained nanocomposite membrane were studied to determine the best method for the adding of nanoparticles in order to obtain a membrane with the minimum fouling and maximum dye separation efficiency.

2. Experimental

2.1. Materials

Polysulfone (PSf) (MW: 75,000 Da) was supplied by Acros Organics and used as a base polymer for membrane (17 wt.%). *N*-methyl-2-pyrrolidone (NMP) was supplied by Merck used as a solvent for polymer (75 wt.%). Poly ethylene glycol (MW: 400 g/mol) was supplied by Merck used as a pore former (8 wt.%). Acrylic acid was supplied by Merck used as an agent for deposition of Al_2O_3 nanoparticles onto the membrane surface. Disperse dyes were supplied by Alvan sabet dye company. The weight ratio of Al_2O_3 to casting solution was considered 0.51 wt.% (equal to 0.03 for Al_2O_3/PSf weight ratio). The composition of casting solution (40.204 g) is presented in Table 1.

2.2. Nanocomposite membrane preparation

2.2.1. Entrapping nanoparticles in polymer structure

Al_2O_3 entrapped PSf ultrafiltraion membranes were prepared by dispersing nano-sized particles

Table 1
Composition of casting solution

Material	Weight in casting solution (g)	Weight ratio in casting solution (%)
PSf	6.800	16.91
PEG	3.200	7.96
NMP	30.00	74.62
Al_2O_3	0.204	0.51

uniformly into NMP solution and was sonicated at 70˚ C for 60 min, and then, PSf was subsequently added under continuous stirring. After adding additive and sonicating again for 60 min, the membrane was cast onto a clean glass plate with 350 μm casting knife and exposed under forced-convection evaporation for 30 s. Then, immediately immersed in a water coagulation bath at 25˚C to form membrane. Two casting solutions were synthesized through mechanical and ultrasonic stirring to study the best method for the dispersion of nanoparticles. In entrapping method, nanoparticle content in casting solution is different depended to nanoparticle type, membrane material and application [9]. According to the literature [9,40], membrane structure and performance is a function of nanoparticle concentration. For any polymeric system (polymer/solvent/nanoparticle), nanoparticle aggregation occurres, when the nanoparticle concentration reaches to a certain level [9,40]. For example, Sotto et al. [40] reported that nanoparticle aggregation for TiO_2/PES systems takes place at 0.2 wt.% TiO_2/casting solution. For nanocomposite membranes containing Al_2O_3 nanoparticles, Maximous et al. [12] examined entrapped membrane with 0.01, 0.03, 0.05 Al_2O_3/PES mass ratios, while Yan et al. [11] considered 0–0.04 Al_2O_3/PVDF weigh ratio. In this study, similar to the aforesaid researches [11,12], Al_2O_3 nanoparticle concentration of 0.03 Al_2O_3/PSf mass ratio (equal to 0.51% Al_2O_3/casting solution) considered.

2.2.2. Deposition of nanoparticles onto the membrane surface by using photopolymerization

Deposition of nanoparticles onto membrane surface is a novel and more efficient method for preparing nanocomposite membranes [9,17,19]. In this work, Al_2O_3-deposited PSf nanofiltraion membranes were prepared in two levels; first, polymeric membranes without nanoparticles casted in the way that mentioned before, second, solution deposition of Al nanoparticles and acrylic acid (6 wt.%) onto the membrane surface by UV-irradiation grafting polymerization technique using a UV lamp shown in Fig. 1 (Philips, UVC, 254 nm wave length, Model TUV8W-G8TS, the Netherlands) at various irradiation time. In this process, poly acrylic acid/nanoparticle layer was deposited on photoactive surface of PSf membrane. Further description about this method was reported in our previous work [41].

2.3. Membrane characterization

2.3.1. Membrane performance

To operate under constant trans-membrane pressure (TMP), membrane filtration was carried out using a stirred batch cell shown in Fig. 2 (Millipore, Amicon, Model No. 8400, USA). The effective membrane area in the dead-end membrane test unit was 41.8 Cm^2 and the applied pressure was fixed at 300 KPa. The performance in constant TMP condition was appropriate to study the fouling behavior.

Following filtration, dye solutions were analyzed using a UV-Visible spectrophotometer (UNICO, Model: s2100, USA). The absorbance of permeates and feed were measured and converted to concentration using an absorbance/concentration calibration curve. The rejection of dye solutions was calculated through Equation (1) [15].

$$R(\%) = (1 - C_p/C_f) \times 100 \quad (1)$$

In Eq. (1), R% represents rejection, while C_f and C_p represent concentration of dye in the feed and concentration of dye in the membrane permeate, respectively.

Table 2 lists the disperse dye used in the experiment and their molecular weights.

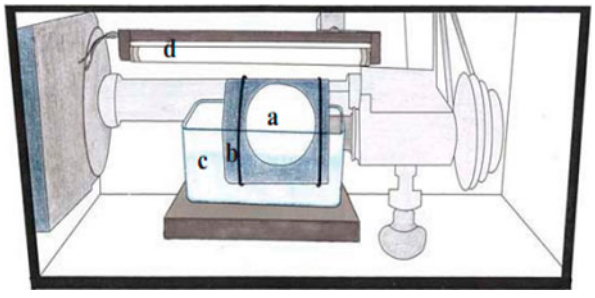

Fig. 1. UV-irradiation chamber including: (a) membrane sample, (b) rotating cylinder, (c) monomer solution and (d) UV-lamp.

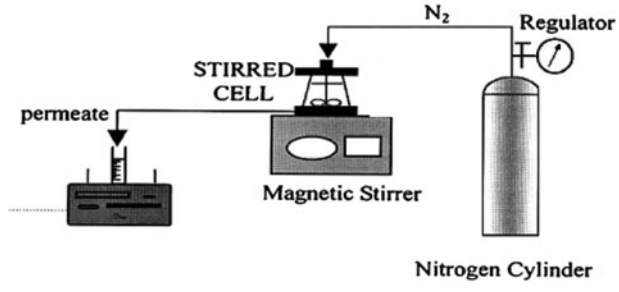

Fig. 2. Schematic diagram of stirred batch cell system [12].

Table 2
Used disperse dye and their properties

Disperse dye	MW (g/mol)	λ_{max} (nm)
Blue 2RLS	639.41	560
Red BRLS	505.91	460
Blue 2RL	459.30	560
Yellow 4GNL	361.74	490

2.3.2. Fourier transform infrared spectrum

Fourier transform infrared (FTIR) spectrum was used to prove the presence of alumina nanoparticles in the structure of PSf membrane (BRUKER, Model: TENSOR 27, Germany). Membrane samples became a little thin and transparent due to the high pressure (14 bar), and then, they were analyzed.

2.3.3. X-ray diffraction (XRD)

X-ray diffraction analysis was used to study the presence and the arrangement of nanoparticles in the structure of polymer (PHILIPS, Type NUM: PW3040/60, Netherlands). The size of nanoparticles inside and outside the membrane structure can be calculated by using XRD results and Eq. (2) (Scherer Equation).

$$t = \frac{k \times \lambda}{\beta \times cos\theta} \quad (2)$$

In Eq. (2), t represents the thickness of crystallite, while k is a constant dependent on crystallite shape (0.89), λ shows the X-ray wavelength, B represents full width at half maximum, and θ is Bragge angle.

3. Results and discussion

3.1. Nanocomposite membrane analysis

3.1.1. FTIR spectrum

Fig. 3 displays FTIR spectrum of alumina nanoparticles, PSf ultrafiltration membrane, and nanocomposite membrane. There are observed a peak in wave number of 3,400 cm^{-1} and another one in 1,600 cm^{-1} in alumina nanoparticles spectrum that are related to –OH and Al–O functional groups of alumina particles, respectively [42]. Comparison between the spectrum of neat PSf membrane and nanocomposite membrane shows a wide peak in the area of 3,000–3,600 cm^{-1}, which confirms the presence of Al_2O_3 nanoparticles in the structure of PSf membrane.

3.1.2. XRD analysis

Fig. 4 demonstrates XRD pattern for PSf membrane, nanocomposite membrane, and alumina nanoparticles. As is seen in Fig. 4, The XRD diffraction pattern of PSf/Al_2O_3 composite membrane has three crystalline characteristic peaks, that is analogous with the characteristic peaks of Al_2O_3 crystal powders in addition to the dispersion peak of amorphous PSf, nevertheless their locations occurs slight shift, compared with the pattern of Al_2O_3 nanoparticles. This shift of characteristic peaks of Al_2O_3 in PSf/Al_2O_3 composite membrane indicates that there may be exist interactions between polymers and Al_2O_3 nanoparticles. It has caused by the mixing of nanoparticles with the polymer structure, and the creation of a uniform

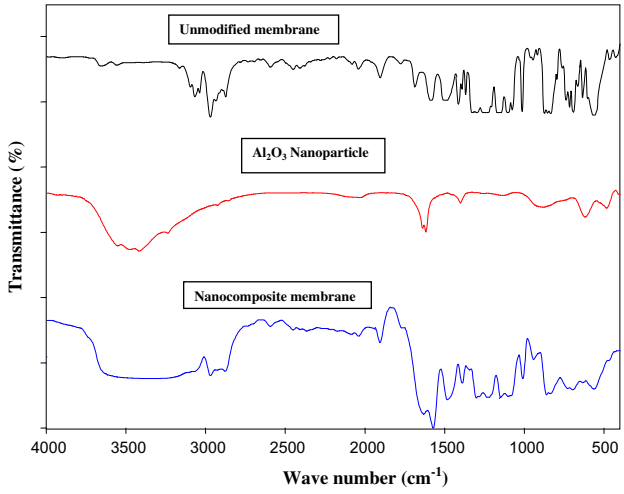

Fig. 3. FTIR Spectrum of Al_2O_3 entrapped PSf ultrafiltration membrane, PSf membrane and Al_2O_3 nanoparticle.

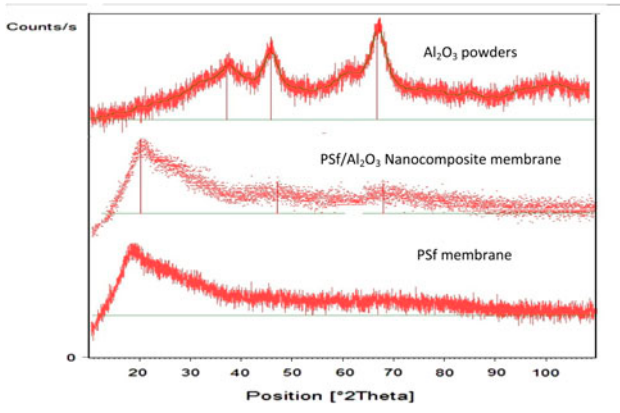

Fig. 4. XRD Pattern of Al_2O_3 Powders, PSf/Al_2O_3 nanocomposite membrane and PSf membrane.

structure [42]. By implementing XRD pattern and by using Scherer Equation, the size of alumina nanoparticles was predicted to be 16.61 nm, and the nanoparticles had a size of 58.3 nm after placement in the polymer structure. The reason for this fact was the nanoparticles aggregation after being placed in the polymer structure.

3.1.3. Measurement of contact angle

Due to their hydrophilic nature, alumina nanoparticles play an important role in the membrane fouling reduction. To study this fact, the water contact angles of all synthesised nanocomposite membranes and polymeric membrane were measured. Table 3 displays the results. According to the results, the hydrophilicity of nanocomposite membranes is higher than polymeric membranes. In addition, the deposited membrane has a more hydrophilic surface in comparison with other nanocomposite membranes. The reason is the presence of nanoparticles and acrylic acid onto the membrane surface. Hydrophilic nature of nanoparticles [9] and the presence of acrylic acid [41] create hydrophilic characteristic onto the membrane surface while in the alumina entrapped membrane, only nanoparticles help the increase in hydrophilicity. Table 3 shows hydrophilicity of other nanocomposite membranes prepared by other researchers as well. According to the results displayed in Table 3, alumina nanoparticles have a better effect on the hydrophilicity of the membrane comparing with TiO_2 nanoparticles.

3.2. Filtration performance

The performance of the synthesized nanocomposite membranes were evaluated in dead-end filtration system and the flux and rejection of disperse dye solutions were calculated. Results showed significant changes in the flux and rejection of nanocomposite membranes in comparison with neat polymeric membranes.

3.2.1. Disperse dyes flux

According to the results shown in Fig. 5, all nanocomposite membranes have a higher flux than polymeric membranes without nanoparticles. As was seen in the analysis of membrane contact angle, the reason is the increase in the hydrophilicity of nanocomposite membranes due to the presence of nanoparticles. As is seen in Fig. 5, nanocomposite membrane with entrapped Al_2O_3 by ultrasonic stirring have the highest flux among the others. The reason can be explained by the better dispersion of the hydrophilic nanoparticles in the structure of this membrane, and consequently, its higher hydrophilicity and more and larger pores comparing to the other three synthesized membranes. This fact has been reported in other researches carried out by different researchers on the effect of nanoparticles on the behavior of PSf membrane [17,18,44–46]. Comparing nanocomposite membranes with entrapped nanoparticles to nanocomposite membranes with coated nanoparticles shows that although the presence of nanoparticles increases the hydrophilicity of the membrane, the creation of a coating of polyacrylic acid and nanoparticles onto the membrane surface result in the reduction in pores size, and consequently, reduction in membrane flux [41].

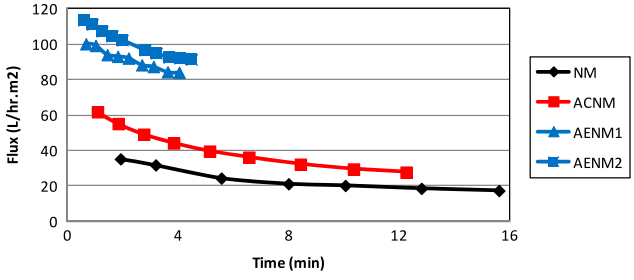

Fig. 5. Flux decreasing performance of neat membrane (NM), Al_2O_3 coated nanocomposite membrane (ACNM) and Al_2O_3 entrapped nanocomposite membrane (AENM) (1: mechanical stirring/2: ultrasonic stirring).

Table 3
Contact angle of NM, ACNM and AENM (1: mechanical stirring/2: ultrasonic stirring).

Membrane type	Contact angle (°)	Contact angle (°) in studies
NM	80	
AENM1	75	84 [16]
AENM2	66	75 [43]
ACNM	46	

Table 4
Filtration data of NM, ACNM and AENM (1: mechanical stirring/2: ultrasonic stirring).

Membrane type	Dye rejection (%)	Increase in dye rejection compared to NM (%)
NM	81.7378	0
AENM1	88.0252	7.68
AENM2	96.4084	17.92
ACNM	100	22.31

3.2.2. Disperse dyes rejection

According to Table 4, dye rejection is higher in nanocomposite membranes than in polymeric membranes. As is seen, the presence of nanoparticles in the structure of membrane not only increases the hydrophilicity and flux, which decreases the fouling, but also improves the separation of disperse dyes. The reason for this behavior can be due to the formation of more number of smaller pores caused by the delay phase inversion due to the presence of nanoparticles. The same behavior has been observed in the studies carried out by other researchers too [9].

Table 4 also presents the increase in rejection efficiency of nanocomposite membrane compared to neat membrane (third column). As is seen in the figure, the membrane with surface deposition has a higher rejection than the membrane with entrapped nanoparticles. The reason can be explained by the smaller size of the membrane pores due to the presence of poly acrylic acid/nanoparticle layer on the membrane surface [41]. It augments the quality of separation up to 22.31% but decreases the flux.

4. Conclusion

In this study, Al_2O_3 nanoparticles were added to PSf ultrafiltration membrane structure through the two methods of entrapment in the structure and surface deposition to study the membrane performance in the filtration of dye solutions. Major findings from this study are:

- Flux decline is less in nanocomposite membranes than in polymeric membranes without nanoparticles the reason is the increase in the hydrophilicity of nanocomposite membranes due to the presence of nanoparticles.
- The flux is higher in nanocomposite membranes with entrapped Al_2O_3 by ultrasonic stirring than in nanocomposite membranes with deposited Al_2O_3. It seems that the structure trapping method and the presence of nanoparticles in the membrane structure is a better method to increase hydrophilicity, and consequently, reducing the fouling.
- Nanocomposite membranes have higher dye rejection in comparison with polymeric membranes. It means the presence of alumina nanoparticles helps the improvement of the quality of disperse dye separation.
- Nanocomposite membrane with surface deposition has a higher rejection than the membrane with entrapped nanoparticles which can be due to decrease in pore size through poly acrylic acid/Al_2O_3 nanoparticle deposition on membrane surface.
- FTIR analysis confirms the presence of alumina nanoparticles in the membrane structure.
- XRD analysis confirms the size of nanoparticles in the polymer structure and also confirms the presence of interactions between Al_2O_3 nanoparticles and PSf. It indicates the effects of nanoparticles on the properties of the polymeric structure.

Acknowledgments

The authors would like to thank Iran Nanotechnology Society (INS) for financial support this study and Ms Sara Rezaee for her kind cooperation during the experimental activity.

References

[1] M. Amini, M. Homayoonfal, M. Arami, A. Akbari, Modification and characterization of prepared polysulfone ultrafiltration membranes via photografted polymerization: Effect of different additives, Desalin. Water Treat. 9 (2009) 43–48.
[2] D. Chen, L.K. Weavers, H.W. Walker, Ultrasonic control of ceramic membrane fouling: Effect of particle characteristics, Water Res. 40 (2006) 840–850.
[3] T. Mohammadi, S.S. Madaeni, M.K. Moghadam, Investigation of membrane fouling, Desalination 153 (2002) 155–160.
[4] P. Pandy, R.S. Chauha, Membrane for gas separation, Prog. Polym. Sci. 26 (2001) 853–893.
[5] I. Genne, S. Kuypers, R. Leysen, Effect of the addition of ZrO_2 to polysulfone based UF membranes, J. Membr. Sci. 113 (1996) 343–350.
[6] P. Aerts, I. Genne, S. Kuypers, R. Leysen, I.F.J. Vankelecom, P.A. Jacobs, Polysulfone–aerosil composite me, branes. Part 2. The influence of the addition of aerosol on the skin characteristics and membrane properties, J. Membr. Sci. 178 (2001) 1–11.
[7] A. Bottino, C. Caparmelli, P. Piaggio, V. D'Asti, Preparation and properties of novel organic–inorganic porous membranes, Sep. Purif. Technol. 22–23 (2001) 269–275.
[8] Z.S. Wang, T. Sasaki, M. Muramatsu, Y. Ebina, T. Tanake, L. Wang, M. Watanabe, Self-assembled multilayers of titania nanoparticles and nanosheets with polyelectrolytes, Chem. Mater. 15 (2003) 807–812.
[9] M. Homayoonfal, M.R. Mehrnia, Y.M. Mojtahedi, A.F. Ismail, Effect of metal and metal oxide nanoparticle impregnation route on structure and liquid filtration performance of polymeric nanocomposite membranes: A comprehensive review, Desalin. Water Treat. (in press), doi: 10.1080/19443994.2012.749055.
[10] J. Kim, B.V. Bruggen, The use of nanoparticles in polymeric and ceramic membrane structures: Review of manufacturing procedures and performance improvement for water treatment, Environ. Pollut. 158 (2010) 2335–2349.
[11] L. Yan, Y.S. Li, C.B. Xiang, S. Xianda, Effect of nano-sized Al_2O_3-particle addition on PVDF ultrafiltration membrane performance, J. Membr. Sci. 276 (2006) 162–167.
[12] N. Maximous, G. Nakhla, W. Wan, K. Wong, Preparation, characterization and performance of Al_2O_3/PES membrane for wastewater filtration, J. Membr. Sci. 341 (2009) 67–75.
[13] J.S. Taurozzi, C.A. Crock, V.V. Tarabara, C_{60}-polysulfone nanocomposite membranes: Entropic and enthapic determinants of C_{60} aggregation and its effects on membrane properties, Desalination 269 (2011) 111–119.

[14] L.H. Li, J.C. Deng, H.R. Deng, Z.L. Liu, L. Xin, Synthesis and characterization of chitosan/ZnO nanoparticle composite membranes, Carbohydr. Res. 345 (2010) 994–998.
[15] S.H. Kim, S.Y. Kwak, B.H. Sohn, T.H. Park, Design of TiO_2 nanoparticle self-assembled aromatic polyamide thin-film-composite (TFC) membrane as an approach to solve biofouling problem, J. Membr. Sci. 211 (2003) 157–165.
[16] X. Cao, J. Ma, X. Shi, Z. Ren, Effect of TiO_2 nanoparticle size on the performance of PVDF membrane, Appl. Surf. Sci. 253 (2006) 2003–2010.
[17] T.H. Bae, T.M. Tak, Effect of TiO_2 nanoparticle on fouling mitigation of ultrafiltration membranes for activated sludge filtration, J. Membr. Sci. 249 (2005) 1–8.
[18] Y. Yang, H. Zhang, P. Wang, Q. Zheng, J. Li, The influence of nano-sized TiO_2 fillers on the morphologies and properties of PSf UF membrane, J. Membr. Sci. 288 (2007) 231–238.
[19] A. Rahimpour, S.S. Madaeni, A.H. Taheri, Y. Mansourpanah, Coupling TiO_2 nanoparticles with UV irradiation for modification of polyethersulfone ultrafiltration membranes, J. Membr. Sci. 313 (2008) 158–169.
[20] J.H. Li, Y.Y. Xu, L.P. Zhu, J.H. Wang, C.H. Du, Fabrication and characterization of a novel TiO_2 nanoparticle self-assembly membrane with improved fouling resistance, J. Membr. Sci. 326 (2009) 659–666.
[21] Y. Mansourpanah, S.S. Madaeni, A. Rahimpour, A. Farhadian, A.H. Taheri, Formation of appropriate sites on nanofiltration membrane surface for binding TiO_2 photo-catalyst: Performance, characterization and fouling-resistant capability, J. Membr. Sci. 330 (2009) 297–306.
[22] M.L. Luo, J.Q. Zhao, W. Tang, C.S. Pu, Hydrophilic modification of poly(ether sulfone) ultrafiltration membrane surface by self-assembly of TiO_2 nanoparticle, Appl. Surf. Sci. 249 (2005) 76–84.
[23] I. Soroko, A. Livingston, Impact of TiO_2 nanoparticles on morphology and perfprmance of crosslinked polyimide organic solvent nanofiltration (OSN) membranes, J. Membr. Sci. 343 (2009) 189–198.
[24] T.H. Bae, T.M. Tak, Preparation of TiO_2 self-assembled polymeric nanocomposite membranes and examination of their fouling mitigation effects in a membrane bioreactor system, J. Membr. Sci. 266 (2005) 1–5.
[25] A. Razmjou, J. Mansouri, V. Chen, The effects of mechanical and chemical modification of TiO_2 nanoparticles on the surface chemistry, structure and fouling performance of PES ultrafiltration membranes, J. Membr. Sci. 378 (2011) 73–84.
[26] S.Y. Lee, H.J. Kim, R. Patel, S.J. Im, J.H. Kim, B.R. Min, Silver nanoparticles immobilized on thin film composite polyamide membrane: Characterization, nanofiltration, antifouling properties, Polym. Adv. Technol. 18 (2007) 562–568.
[27] H.L. Yang, J.C.T. Lin, C. Huang, Application of nanosilver surface modification to RO membrane and spacer for mitigating biofouling in seawater desalination, Water Res. 43 (2009) 3777–3786.
[28] K. Zodrow, L. Brunet, S. Mahendra, D. Li, A. Zhang, Polysulfone ultrafiltration membranes impregnated with silver nanoparticles show improved biofouling resistance and virus removal, Water Res. 43 (2009) 715–723.
[29] J.S. Taurozzi, H. Arul, V.Z. Bosak, A.F. Burban, T.C. Voice, M.L. bruening, V.V. Tarabara, Effect of filler incorporation route on the properties of polysulfone–silver nanocomposite membranes of different porosities, J. Membr. Sci. 325 (2008) 58–68.
[30] A. Bottino, G. Capannelli, A. Comite, Preparation and characterization of novel porous PVDF–ZrO_2 composite membranes, Desalination 146 (2002) 35–40.
[31] N. Maximous, G. Nakhla, W. Wan, K. Wong, Performance of a novel ZrO_2/PES membrane for wastewater filtration, J. Membr. Sci. 352 (2010) 222–230.
[32] S.H. Chen, R.M. Liou, C.L. Lai, M.Y. Hung, M.H. Tsai, S.L. Huang, Emstructureded nano-iron polysulfone membrane for dehydration of the ethanol/water mixtures by pervaporation, Desalination 234 (2008) 221–231.
[33] J. Xu, D. Bhattacharyya, Fe/Pd nanoparticle immobilization in microfiltration membrane pores: Synthesis, characterization, and application in the dechlorination of polychlorinated biphenyls, Ind. Eng. Chem. Res. 46 (2007) 2348–2359.
[34] J. Ahn, W.J. Chung, I. Pinnau, M.D. Guiver, Polysulfone/silica nanoparticle mixed-matrix membranes for gas sepsration, J. Membr. Sci. 314 (2008) 123–133.
[35] A. Bottino, G. Capannelli, V. D'Asti, P. Piaggio, Preparation and properties of novel organic–inorganic porous membranes, Sep. Purif. Technol. 22–23 (2001) 269–275.
[36] A.L. Ahmad, M.A. Majid, B.S. Ooi, Functionalized PSf/SiO_2 nanocomposite membrane for oil-in-water emulsion separation, Desalination 268 (2011) 266–269.
[37] Yu. Zhang, L. Shan, Z. Tu, Ya. Zhang, Preparation and characterization of novel Ce-doped nonstoichiometric nanosilica polysulfone composite membranes, Sep. Purif. Technol. 63 (2008) 207–212.
[38] S. Yu, X. Zuo, R. Bao, X. Xu, J. Wang, J. Xu, Effect of SiO_2 nanoparticle addition on the characteristics of a new organic–inorganic hybrid membrane, Polymer 50 (2009) 553–559.
[39] P. Jian, H. Yahui, W. Yang, L. Linlin, Preparation of polysulfone–Fe_3O_4 composite ultrafiltration membrane and its behavior in magnetic field, J. Membr. Sci. 284 (2006) 9–16.
[40] A. Sotto, A. Boromand, R. Zhang, P. Luis, J.M. Arsuaga, J. Kim, B. Van der Bruggen, Effect of nanoparticle aggregation at low concentrations of TiO_2 on the hydrophilicity, morphology, and fouling resistance of PES–TiO_2 membranes, J. Colloid Interf. Sci. 363 (2011) 540–550.
[41] M. Homayoonfal, A. Akbari, M.R. Mehrnia, Preparation of polysulfone nanofiltration membranes by UV-assisted grafting polymerization for water softening, Desalination 263 (2010) 217–225.
[42] T.M.H. Costa, M.R. Gallas, E.V. Benvenuetti, J.A.H. Da Jornada, Study of nanocrystalline γ-Al_2O_3 produced by high-pressure compaction, J. Phys. Chem. 103 B (1999) 4278–4284.
[43] J.B. Li, J.W. Zhu, M.Sh. Zheng, Morphologies and properties of poly(phthalazinone ether sulfone ketone) matrix ultrafiltration membranes with entrapped TiO_2 nanoparticles, J. Appl. Polym. Sci. 103 (2007) 3623–3629.
[44] Y. Yang, P. Wang, Preparation and characterizations of a new PSf/TiO_2 hybrid membranes by sol–gel process, Polymer 47 (2006), 2683-268.
[45] Y. Yang, J. Wu, Q. Zheng, X. Chen, H. Zhang, The research of rheology and thermodynamics of organic–inorganic hybrid membrane during the membrane formation, J. Membr. Sci. 311 (2008) 200–207.
[46] I. Genne, S. Kuypers, R. Leysen, Effect of the addition of ZrO_2 to polysulfone based UF membranes, J. Membr. Sci. 113 (1996) 343–350.